Journal of Modern Optics

ISSN: 0950-0340 (Print) 1362-3044 (Online) Journal homepage: http://www.tandfonline.com/loi/tmop20

Acousto-optic displacement-measuring interferometer: a new heterodyne interferometer with Ångstrom-level periodic error

Tony Schmitz & John Beckwith

To cite this article: Tony Schmitz & John Beckwith (2002) Acousto-optic displacement-measuring interferometer: a new heterodyne interferometer with Ångstrom-level periodic error, Journal of Modern Optics, 49:13, 2105-2114, DOI: 10.1080/09500340210123938

To link to this article: https://doi.org/10.1080/09500340210123938

Published online: 03 Dec 2010.

JOURNAL OF MODERN OPTICS, 2002, VOL. 49, NO. 13, 2105–2114

Acousto-optic displacement-measuring interferometer: a new heterodyne interferometer with Ångstrom-level periodic error

TONY L. SCHMITZ†‡

Manufacturing Metrology Division, National Institute of Standards and Technology, Gaithersburg, Maryland 20899, USA; e-mail: tony.schmitz@nist.gov

and JOHN F. BECKWITH§

Electronics Engineering Technologies Division, Lawrence Livermore National Laboratory, Livermore, California 94550, USA

(*Received 15 March 2001; revision received 17 October 2001*)

Abstract. A concept for a new displacement-measuring interferometer has been developed. The motivation behind this work is minimization of the periodic error caused by unwanted leakage between the two frequencies in commercially available heterodyne systems. Typically, the two frequencies are carried on a single beam and separated by polarization-dependent optics. Imperfect optics, non-ideal laser heads and mechanical misalignment may cause each frequency to be leaked into both the reference and the measurement paths, ideally consisting of a single light frequency. The new polarization-independent interferometer described here uses an acousto-optic modulator as the beam splitter and eliminates the frequency leakage by spatially separating the two light beams. Bench-top experiments have shown a reduction in periodic error to 0.18 nm (1.8 Å). The device description, as well as suggestions for simple architecture implementations, are presented.

1. Introduction

Periodic error in heterodyne displacement-measuring interferometry has been carefully examined in technical literature. Several researchers have identified and modelled sources of the nonlinearity in traditional Michelson-type heterodyne interferometers [1–27]. Additionally, experimental configurations have been described which minimize or eliminate the periodic error inherent in these systems (see, for example [8, 16, 19, 28]). Although these methods have been successfully implemented, they typically require complex mechanical and/or electrical manipulations and are generally absent from commercial implementations. A new

† Research completed at Lawrence Livermore National Laboratory, Livermore, California 94550, USA.

‡ Author for correspondence.

§ Retired.

Journal of Modern Optics ISSN 0950–0340 print/ISSN 1362–3044 online
http://www.tandf.co.uk/journals
DOI: 10.1080/09500340210123938

concept for a heterodyne interferometer that minimizes periodic error, while maintaining a simple architecture, is described here.

2. Background

A fundamental source of systematic error in Michelson-type heterodyne interferometers is unwanted leakage of each of the two polarization-coded light frequencies into both the measurement and the reference paths. In a perfect system, a single wavelength would travel to a fixed reference target, while a second single wavelength travelled to a moving target. Interference of the combined signals would yield a perfectly sinusoidal trace with a phase that varied, relative to a reference phase signal, in response to motion of the moving target. However, the inherent frequency leakage of the two signals in actual implementations produces an interference, or beat, signal which is not exactly sinusoidal (i.e. contains spurious spectral content) and leads to a periodic, or non-cumulative, error in the measured displacement.

Experimental and analytical analyses of measurement signal frequency content have identified both first- and second-harmonic periodic errors, or errors of one and two cycles per wavelength of optical path change respectively. Physically, these errors arise from frequency leakage in the laser source (non-orthogonality between the two frequencies exiting the laser head and ellipticity of the ideally linear output polarizations), non-ideal optical components (imperfect extinction between the two polarizations in the polarizing beam splitter and retroreflector polarization rotation), mechanical misalignment of the interferometer (e.g. roll of the laser coordinate system with respect to the interferometer), parasitic reflections and two-tone intermodulation distortions in the amplifying electronics.

The set-up for a typical, commercially available single pass heterodyne interferometer is shown in figure 1. Owing to leakage, each optical frequency may be present in both the reference and the measurement paths of the interferometer. Detection of the interference signal during constant-velocity motion of the measurement retroreflector exhibits multiple spectral peaks if this leakage exists. The desired ac interference measurement signal is seen at a frequency equal to the beat frequency (i.e. the difference between the two optical source frequencies f_b) up or

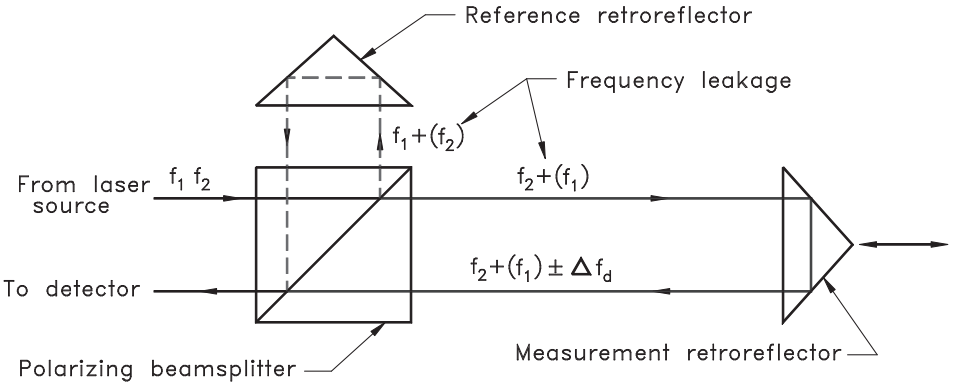

Figure 1. Traditional heterodyne interferometer set-up.

down-shifted, depending on target direction, by a scalar amount proportional to the velocity of the moving retroreflector (i.e. the Doppler shift Δf_d). With good alignment of the measurement beam and axis motion, the measurement signal amplitude will effectively remain constant during motion of the moving retroreflector. Also present, however, will be spectral content that essentially remains at the beat frequency, known as spatial first-harmonic or *ac reference* terms, and a peak upshifted or downshifted from the beat frequency by an amount equal to but opposite from the measurement signal frequency shift, referred to as the second-harmonic or leakage-induced *ac interference* term (figure 2). *Optical power* terms may also be observed at zero frequency and *dc interference* terms at $+\Delta f_d$ in fully leaking configurations, when each source frequency exists in both the measurement and the reference paths. However, for low target velocities and the typical phase-locked loop modulation bandwidths associated with phase measuring electronics in commercially available systems, it is the ac reference and leakage-induced ac interference terms that generally dominate the periodic error magnitude. The attenuation of these error signals with respect to the measurement signal determines the peak-to-peak value of the resulting periodic error. Reported values range approximately from 0.4 to 12 nm.

3. Concept description

The new displacement-measuring interferometer (DMI) does not rely on polarization coding and polarization-dependent optics to separate and recombine the reference and measurement frequencies of the heterodyne system. Instead, the two frequencies originate from an acousto-optic modulator (AOM) and remain spatially separated in the interferometer. The original and frequency-shifted beams travel to reference and measurement retroreflectors respectively, return parallel and collinear to the original path and then recombine in the AOM. No other optical components are required. Because the measurement and reference beams are separated and recombined in the AOM, it serves the function of the polarization beam splitter in typical heterodyne interferometers without introducing the leakage-induced periodic errors described previously.

Figure 3 shows a schematic diagram of the AOM DMI concept. Light from a single frequency stabilized laser source at the optical frequency f_0 is incident on an

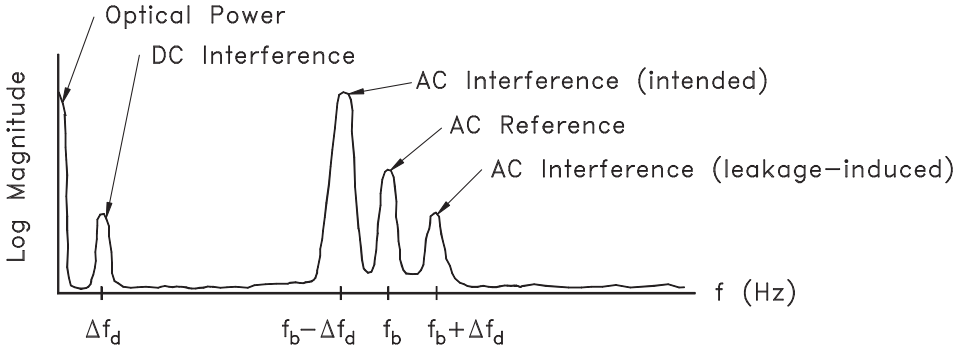

Figure 2. Heterodyne interferometer frequency spectrum for low-velocity target motion.

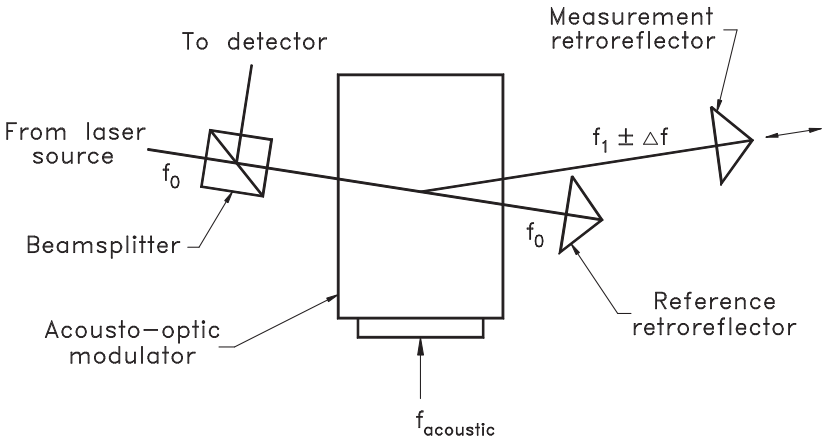

Figure 3. AOM DMI concept.

AOM to produce two beams: the original beam, as well as a diffracted beam with a frequency equal to the sum of the optical and acoustic frequencies, $f_1 = f_0 + f_{\text{acoustic}}$. The f_0 beam then travels to the fixed reference surface, while the f_1 beam is incident on the measurement surface. These beams return along parallel paths respectively and interfere within the AOM. The phase information regarding measurement retroreflector displacement (in the measurement beam direction) is now carried on the interfered signal and travels to a suitable detector. In the figure, a non-polarizing beam splitter is shown which directs the measurement signal to the detector; however, it is not a critical component in the operation of the device.

The technique of spatially separating two measurement beams was first described by Whitman and Korpel [29] and implemented by Cretin *et al*. [19] to measure surface acoustic waves in solids. These applications were concerned with the measurement of acoustic surface perturbations (i.e. the interaction of bulk sound waves with surfaces) in areas such as acoustic holography, ultrasonic surface wave devices and acoustic trapped energy resonators. Additionally, Tanaka *et al*. [16] and Wu *et al*. [28] both described interferometers that use two AOMs to generate the two heterodyne frequencies with one frequency originating from each AOM. These two beams then travel to modified Michelson interferometers.

3.1. *Experimental results*

An initial proof of concept for the AOM DMI has been completed. The experimental set-up is shown in figure 4. Light from a single-frequency stabilized laser source ($f_0 = 473.6122 \times 10^{12}$ Hz; $\lambda_0 = 632.9914$ nm) was first incident on an isolating AOM with a driving frequency f_1 of 65.5 MHz. The function of this AOM was to frequency shift any back-reflected light before it entered the laser tube and avoid destabilization of the source.

The upshifted light next passed through a non-polarizing beam splitter. In this test set-up, the beam splitter was necessary to direct the interference signal to the optical detector. The light was then incident on the AOM interferometer operating at a driving frequency f_2 of 45.5 MHz. At the second AOM, the frequency-shifted beam from the isolating AOM was diffracted into two components. The zeroth

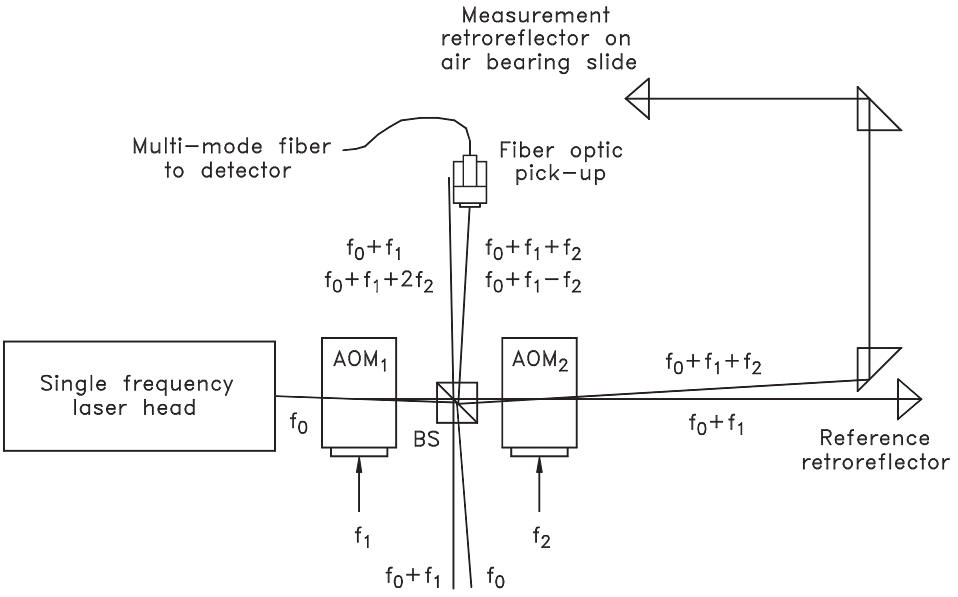

Figure 4. AOM DMI proof-of-concept set-up: BS, beam splitter.

order component, of frequency $f_0 + f_1$, travelled to the reference retroreflector and the first-order component, of frequency $f_0 + f_1 + f_2$, travelled to the moving retroreflector. Because the angle between the two beams exiting the second AOM was small (less than 2 mrad), it was necessary to allow the light to travel approximately 1.5 m before adequate spatial resolution was available to pick off the measurement beam and direct it toward the measurement retroreflector, which was mounted on an air bearing slide.

Once the two beams had travelled individually to the reference and measurement retroreflectors, they interfered during the return path through the AOM. However, because they were still oriented at the Bragg angle they were each frequency shifted. The reference beam was diffracted into two components: zeroth order unchanged and first order downshifted. Similarly, the measurement beam was split into two components: zeroth order unchanged and first order upshifted. Therefore, two individual interference signals were available, each with a beat frequency of two times the AOM interferometer driving frequency, or $2f_2 = 2 \times 45.5 = 91$ MHz.

One of the two available 91 MHz interference signals (the interference of the $f_0 + f_1 + f_2$ measurement and $f_0 + f_1 - f_2$ downshifted reference signals was arbitrarily selected) was launched into a fibre-optic pick-up and carried to a wide bandwidth (dc-1 GHz) receiver by a multimode fiber. The receiver signal was then input to a model 8566B† Hewlett–Packard spectrum analyser with a bandwidth range 100 Hz–22 GHz. The local spectral response was recorded for two cases: case

† Commercial equipment is identified in order to specify certain procedures adequately. In no case does such identification imply recommendation or endorsement by the National Institute of Standards and Technology, nor does it imply that the equipment identified is necessarily the best available for the purpose.

1, no motion of the measurement retroreflector; case 2, 0.128 ms^{-1} measurement retroreflector velocity.

Figure 5 displays the spectrum for case 1 (10 dB/division vertical scale, 91 MHz centre frequency and 2 MHz span horizontal scale). The static 91 MHz beat frequency is seen with the noise floor attenuated by 55 dB. In figure 6, which is plotted with the same scale, the case 2 result shows a 0.42 MHz shift of the

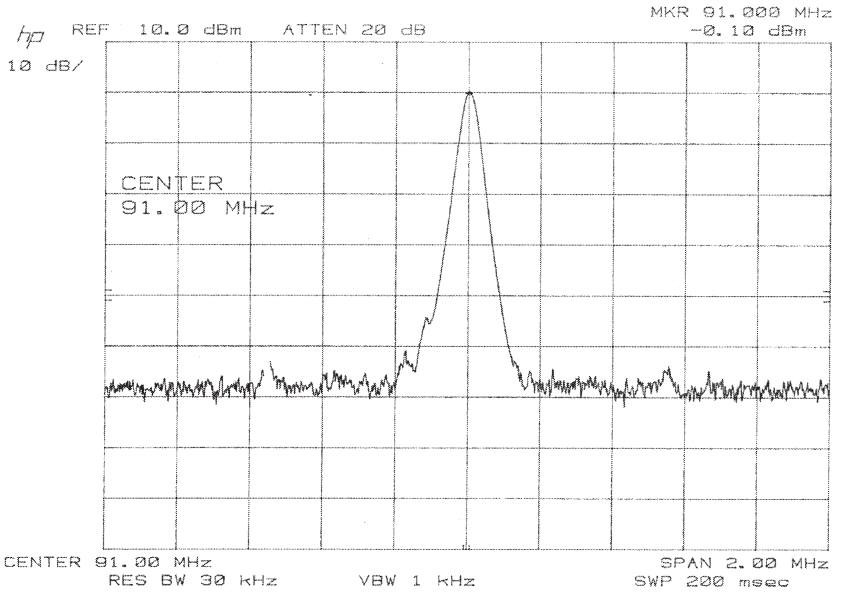

Figure 5. Case 1 spectrum of interference signal (measurement retroreflector at rest).

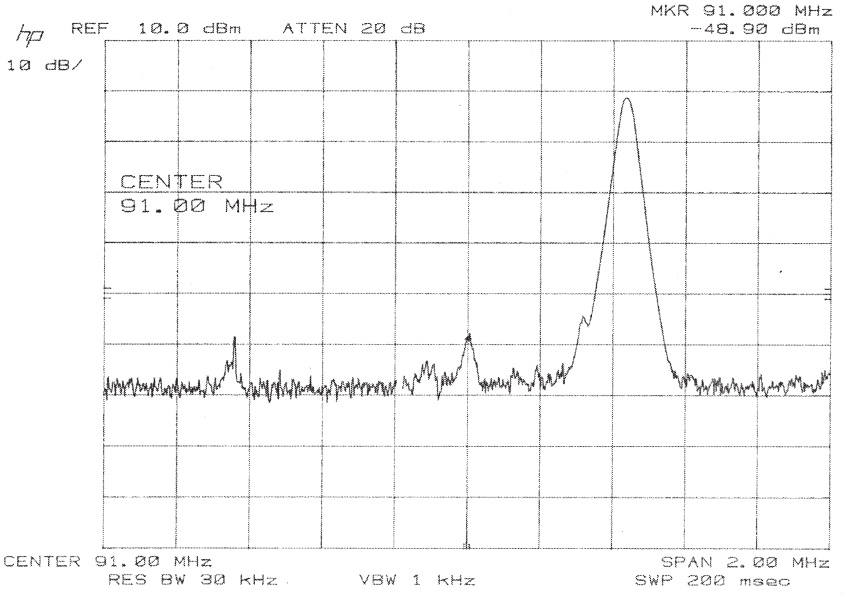

Figure 6. Case 2 spectrum of interference signal (measurement retroreflector moving at 0.128 $m\,s^{-1}$).

measurement signal corresponding to the 0.128 m s^{-1} slide motion for a single-pass interferometer. Content is also recognized at the original beat frequency suggesting a first-order periodic error. However, this signal is attenuated by 48.8 dB with respect to the original measurement signal and represents a non-cumulative error δx of only 0.18 nm:

$$\delta x = \frac{\lambda_0}{\mathrm{FF}} \frac{10^{-\Delta \mathrm{dB}/20}}{2\pi} = \frac{632.9914}{2} \frac{10^{-48.8/20}}{2\pi} = 0.18\,\mathrm{nm}. \tag{1}$$

where FF is the interferometer fold factor. This error is attributed to multiple diffractions, or intermodulations due to reflected acoustic waves, within the AOM.† No appreciable second-order periodic error frequency content is seen.

The combined standard uncertainty u_c, in this periodic error value may be determined according to the *law of propagation of uncertainty* [30]. The variance u_c^2 in a measured value may be obtained by first calculating the partial derivatives of the functional relationship between the measurand δx and input parameters λ_0 and ΔdB with respect to each input, then multiplying the partial derivatives by the standard uncertainty in the associated input (zero covariance between input quantities has been assumed) and, finally, summing the squares of each product:

$$\begin{aligned} u_c^2(\delta x) &= \left(\frac{\delta f}{\delta \lambda_0} u(\lambda_0)\right)^2 + \left(\frac{\delta f}{\delta \Delta \mathrm{dB}} u(\Delta \mathrm{dB})\right)^2 \\ &= \left(\frac{10^{-\Delta \mathrm{dB}/20}}{4\pi} u(\lambda_0)\right)^2 + \left(\frac{-\lambda_0 \ln(10) \times 10^{-\Delta \mathrm{db}/20}}{80\pi} u(\Delta \mathrm{dB})\right)^2 \\ &= 0.01^2\,\mathrm{nm}^2. \end{aligned} \tag{2}$$

For standard uncertainties of 6×10^{-6} nm in wavelength (0.01 ppm) and 0.5 dB in amplitude, the combined standard uncertainty in the periodic error measurement result is 0.01 nm (0.1 Å). The reader may note that this value reflects the uncertainty in the periodic error computed from the spectrum analyser signal alone. Further signal corruption, which could be imposed by the phase-measuring electronics, for example, is highly system dependent and is not considered here.

3.2. *Concept conclusions*

The proof-of-concept set-up verified the possibility of using an AOM as a polarization-independent interferometer. The interference signal demonstrated 48.8 dB attenuation between the measurement signal and first-order periodic error on a bench-top set-up with no external technique for reducing the system nonlinearity and a mechanical slide for motion generation (typical experimental set-ups use a vacuum cell, for example). The proof-of-concept results were, therefore, encouraging. However, the AOM DMI did exhibit a first-order phase error, attributed to bidirectional acoustic interactions within the AOM, with a resulting periodic error of 0.18 nm (1.8 Å). Although this was not a desired result, the AOM interferometer does present a 2–24 times decrease in the periodic error

† This conclusion was supported by analysing the spectrum of the beams exiting the second AOM; content was recorded at both 91 and 131 MHz ($2f_1 = 2 \times 65.5 = 131$ MHz), as well as multiples of these frequencies (i.e. $4f_1$, $4f_2$, etc.).

associated with commercial interferometers while maintaining a simple architecture.

3.3. *Application considerations*

There are several benefits associated with the practical application of this concept, aside from the decreased periodic error. First, with respect to the required equipment, a single-frequency laser source is used rather than a more complex and expensive two frequency laser head, fewer optical components are required, and only one photoreceiver per multiple axis system is necessary. The latter is accomplished by using different AOM driving frequencies in each axis. Second, single-mode fibre feed to each axis allows easy set-up and alignment of a miniaturized package. Third, fibre launching of the light is simplified since polarization-maintaining fibre is not necessary for the polarization-independent interferometer. These benefits are shown graphically in figures 7 and 8. Figure 7 shows the minimum required equipment and set-up for a commercially available three-axis system which could, for example, be used to monitor the axis motions on a precision cutting machine. Figure 8 shows a schematic diagram of a single axis implementation of the AOM DMI. This could be extended to multiple axes by launching the light from the source laser into a single mode fibre and using fibre splitters to separate the light into multiple channels, each of which could travel to a separate AOM operating at a unique driving frequency.

The primary difficulty in implementing the AOM interferometer is adequate spatial separation of the measurement and reference beams given the small diffraction angle encountered in typical commercially available AOMs. Two initial concepts, which seek to overcome this difficulty, are suggested in figures 9 and 10. In figure 9, a simple optical configuration is used to derive two beams, one offset

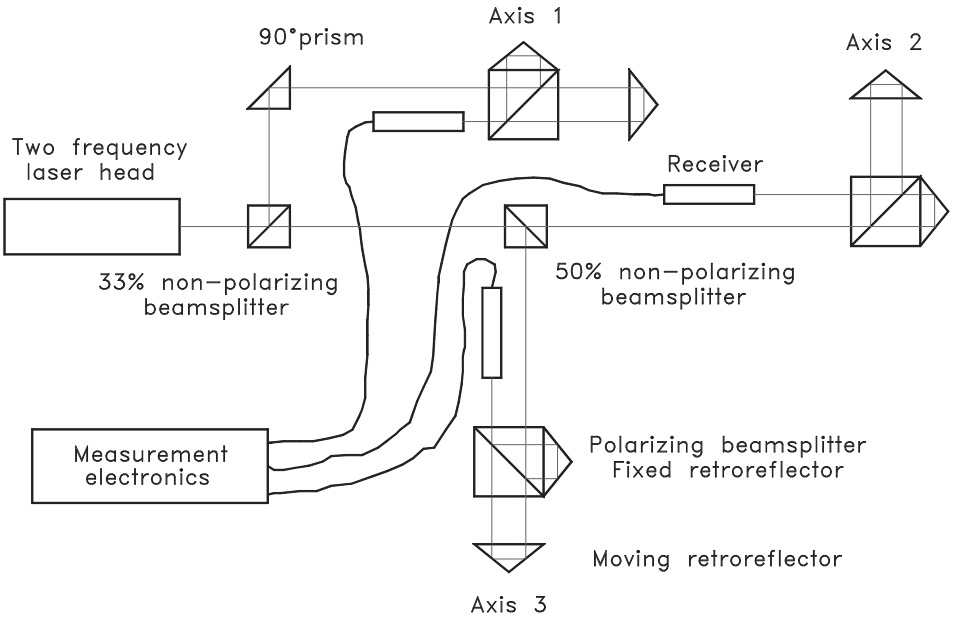

Figure 7. Minimum required hardware for commercial three-axis set-up.

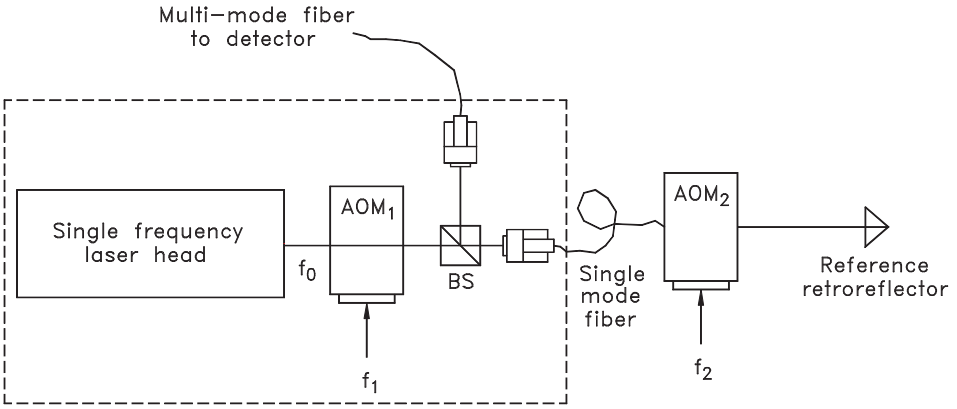

Figure 8. Required hardware for single-axis AOM DMI: BS, beam splitter.

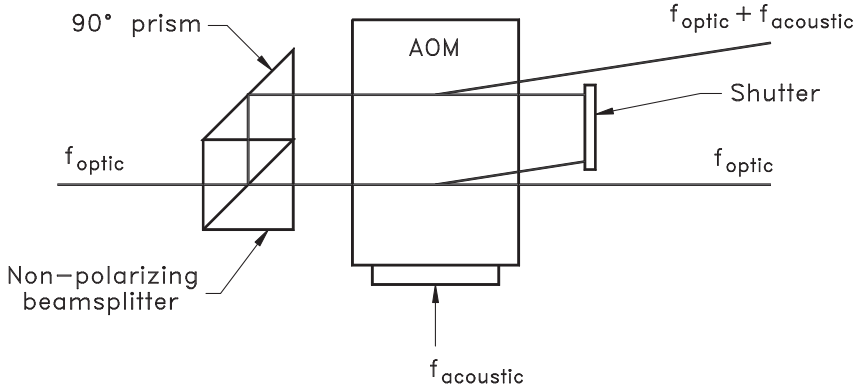

Figure 9. Application concept 1 for the AOM DMI, demonstrating the method to separate measurement and reference beams.

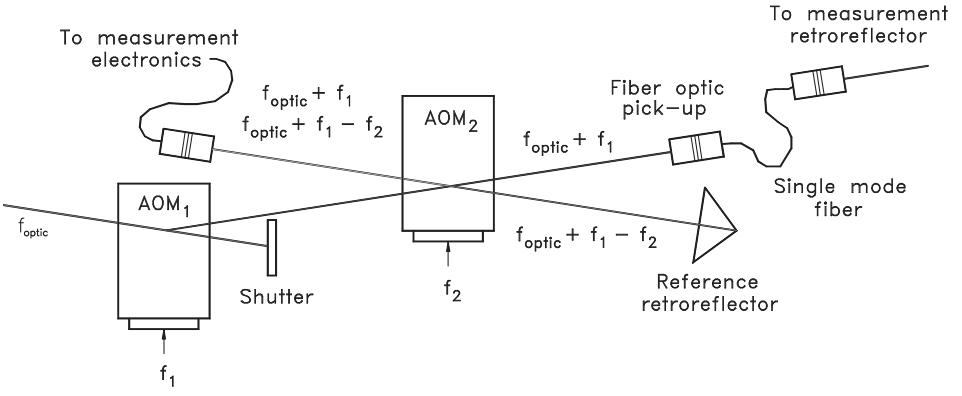

Figure 10. Application concept 2 for the AOM DMI, demonstrating the method to separate measurement and reference beams.

from the other. A possible fault with this design is that the non-polarizing beam splitter and 90° prism are now part of the optical path; additionally, a significant portion of the available laser power is lost. Figure 10 shows a two-AOM configuration with single mode fibre launch. Optical power may also be a consideration here.

4. Conclusions

A new concept for a heterodyne Michelson-type interferometer that minimizes periodic error by eliminating frequency leakage is described. The new interferometer uses an AOM as the beam splitter–recombiner and is polarization independent. A proof of concept for the AOM DMI was developed and successful experimental results presented. These included the demonstration of a 0.18 nm periodic error in a bench-top set-up. Application considerations for the new device are also provided.

References

[1] Fedotova, G., 1980, *Measurement Techniques*, **23,** 577.
[2] Quenelle, R., 1983, *Hewlett-Packard Journal*, **34,** 10.
[3] Sutton, C., 1987, *J. Phys.* E, **20,** 1290.
[4] Barash, V., and Fedotova, G., 1984, *Measurement Techniques*, **27,** 50.
[5] Bobroff, N., 1987, *Appl. Optics*, **26,** 2676.
[6] Rosenbluth, A., and Bobroff, N., 1990, *Precision Engng*, **12,** 7.
[7] Stone, J., and Howard, L., 1998, *Precision Engng*, **22,** 220.
[8] Patterson, S., and Beckwith, J., 1995, *Proceedings of the Eighth International Precision Engineering Seminar*, Compiegne, France, 1995, pp. 101–104.
[9] Badami, V., and Patterson, S., 2000, *Precision Engng*, **24,** 41.
[10] Badami, V., and Patterson, S., 1997, *Proceedings of the 12th Annual American Society for Precision Engineering Conference*, Norfolk, Virginia, 5–10 October 1997, pp. 153–156.
[11] Wu, C., and Deslattes, R., 1998, *Appl. Optics*, **37,** 6696.
[12] Wu, C., and Su, C., 1996, *Measurement Sci. Technol.*, **7,** 62.
[13] Hou, W., and Wilkening, G., 1992, *Precision Engng*, **14,** 91.
[14] Hou, W., and Zhao, X., 1994, *Precision Engng*, **16,** 25.
[15] Howard, L., and Stone, J., 1995, *Precision Engng*, **12,** 143.
[16] Tanaka, M., Yamagami, T., and Nakayama, K., 1989, *IEEE Trans. Instrumentation Measurement*, **38,** 552.
[17] Bobroff, N., 1993, *Measurement Sci. Technol.*, **4,** 907.
[18] Steinmetz, C., 1990, *Precision Engng*, **12,** 12.
[19] Cretin, B., Xie, W., Wang, S., and Hauden, D., 1988, *Optics Commun.*, **65,** 157.
[20] Petru, F., and Cip, O., 1999, *Precision Engng*, **23,** 39.
[21] Augustyn, W., and David, P., 1990, *J. Vac. Sci. Technol.* B, **8,** 2032.
[22] Xie, Y., and Yu, Y., 1992, *Appl. Optics*, **31,** 881.
[23] De Freitas, J., and Player, M., 1993, *Measurement Sci. Technol.*, **4,** 1173.
[24] De Freitas, J., and Player, M., 1995, *J. mod. Optics*, **42,** 1875.
[25] De Freitas, J., 1997, *Measurement Sci. Technol.*, **8,** 1356.
[26] Li, B., and Liang, J., 1997, *Appl. Optics*, **36,** 3668.
[27] Park, B., Eom, T., and Chung, M., 1996, *Appl. Optics,* **35,** 4372.
[28] Wu, C., Lawall, J., and Deslattes, R., 1999, *Appl. Optics*, **38,** 4089.
[29] Whitman, R., and Korpel, A., 1969, *Appl. Optics*, **8,** 1567.
[30] Taylor, B., and Kuyatt, C., 1994, NIST Technical Note 1297, National Institute of Standards and Technology, Gaithersburg, Maryland.